Article

Discovery Medicine 2025; 37(201): 2400–2410
https://doi.org/10.24976/Discov.Med.202537201.203

The Therapeutic Effect of siRNA Formulation That Inhibits Vascular Endothelial Growth Factor on Retinal Neovascularization

Li Li[1,2], Huanzhang Xia[1,*]

[1]School of Life Sciences and Biopharmaceuticals, Shenyang Pharmaceutical University, 110016 Shenyang, Liaoning, China
[2]Shenyang Xingqi Pharmaceutical Co., Ltd., 110163 Shenyang, Liaoning, China
*Correspondence: hzxia@syphu.edu.cn (Huanzhang Xia)
Submitted: 14 July 2025 Revised: 4 September 2025 Accepted: 9 September 2025 Published: 20 October 2025

Background: With growing age and the development of metabolic diseases, the incidence of fundus diseases, including age-related macular degeneration (AMD), pathological myopia, and diabetic retinopathy, has risen sharply, often resulting in the formation of abnormal neovascularization and damage to normal fundus tissue. Anti-vascular endothelial growth factor (VEGF) therapy has emerged as the standard treatment for neovascular fundus diseases. Although the emergence of small interfering RNA (siRNA) drugs targeting VEGF offers a new treatment option for patients with ocular vascular diseases, the requirement of frequent injection and potential safety challenges associated with their administration impose substantial burdens and risks to patients.
Objective: This study aims to develop a simple and straightforward siRNA-based formulation for intraocular injection and assess its efficacy and safety profile.
Methods: This study developed siRNA-based formulations, evaluated the VEGF inhibitory effect, and Half-maximal Inhibitory Concentration (IC_{50}) values at the mRNA level using quantitative reverse transcription polymerase chain reaction (qRT-PCR). Cell viability and proliferation activity were determined using the cell counting kit-8 (CCK-8). Furthermore, the angiogenic capability of the cells was assessed using a tube formation assay. Additionally, a laser-induced mouse choroidal neovascularization (CNV) model was applied to investigate the therapeutic effect of siRNA on retinal neovascularization *in vivo*, and intraocular safety was evaluated using slit lamp examination and hematoxylin and eosin (H&E) staining of retinal tissue sections.
Results: siRNA formulation effectively silenced VEGF expression in human umbilical vein endothelial cells (HUVECs), indicating an mRNA inhibition rate of >85%. The treatment substantially inhibited HUVEC proliferation (compared to the control group: at 24 hours post-administration, siRNA 75 nM and 100 nM groups, $p < 0.05$; at 48 hours, siRNA 50 nM group, $p < 0.05$, and siRNA 75 nM and 100 nM groups, $p < 0.005$; at 72 hours, siRNA 50 nM group, $p < 0.01$, siRNA 75 nM and 100 nM groups, $p < 0.005$). Furthermore, siRNA formulations significantly suppressed angiogenesis compared to the control group (siRNA 50 nM, $p < 0.05$; siRNA 75 nM and 100 nM, $p < 0.01$). Moreover, after a single intravitreal injection, VEGF expression suppressed for up to 5 weeks, along with reduction in neovascularization area compared to the negative control group: at day 7 after administration, medium dose, $p < 0.05$ and high dose, $p < 0.01$; at day 21 after administration, low-, $p < 0.05$, medium dose and high-dose, $p < 0.005$; at day 35 post-administration, low-dose, $p < 0.05$, medium dose, $p < 0.01$, and high-dose, $p < 0.005$. Notably, no significant retinal toxicity was observed in normal rabbits after 3 months of vitreous injection.
Conclusion: This study confirms the therapeutic potential of VEGF-targeting siRNA formulations for retinal diseases, emphasizing their significance in promoting the clinical translation of siRNA-based therapies in ophthalmology.

Keywords: inhibition of vascular endothelial growth factor; siRNA; retinal neovascularization; delivery system

Introduction

Vasculogenesis and angiogenesis play a crucial role in embryonic development. Pathological neovascularization in ocular tissues can lead to vision-threatening vascular diseases, including proliferative diabetic retinopathy, retinal vein occlusion, retinopathy of prematurity, choroidal neovascularization, and corneal neovascularization [1]. Age-related macular degeneration (AMD) develops when extracellular deposits accumulate in the outer retina, ultimately leading to photoreceptor degeneration and central vision loss [2]. The incidence of retinal diseases increases sharply with the progression of metabolic conditions [3]. AMD impacts about 8.7%–11.3% of individuals over 65 years of age, while diabetic retinopathy affects 103 million people worldwide [4]. However, evidence suggests that this number is anticipated to reach approximately 288 million by 2040 [5].

Central to AMD pathology is the pathological overexpression of vascular endothelial growth factor (VEGF). VEGF is primarily synthesized and secreted in the eye by retinal pigment epithelial cells, pericytes, endothelial cells,

glial cells, and ganglion cells [6]. An abnormal increase in VEGF can cause hyperpermeability and neovascularization in the macular area. The expression and regulation of VEGF are strongly associated with the occurrence and progression of several ophthalmic diseases. Particularly, proliferative ocular vascular diseases, such as retinopathy of prematurity (ROP), AMD, and diabetic retinopathy, are all implicated by excessive VEGF-mediated neovascular proliferation. The leakage of these newly produced blood vessels can lead to macular swelling and tissue damage, and subsequently form fibrous scars, resulting in substantial vision impairment. VEGF plays a crucial role in angiogenesis [7], and VEGF-A is a critical subtype, which is involved in the modulation of both physiological homeostasis and pathological angiogenic processes. Furthermore, VEGF-A has been recognized as a key contributor to tumor growth and metastasis [8].

To alleviate these retinal injuries, medical science has advanced in developing and continuously improving anti-VEGF therapies. The primary goal of anti-VEGF therapy is to reduce exudation and edema, thereby stabilizing or improving visual acuity. Currently, anti-VEGF therapy has become the standard of care and treatment for neovascular retinal lesions. Intravitreal anti-vascular endothelial growth factor (VEGF) therapies, such as ranibizumab, aflibercept, and unlicensed bevacizumab, are considered the gold standard for the treatment of neovascular age-related macular degeneration (nAMD), slowing the pathophysiological progression and reducing the severity of vision loss [9]. Although anti-VEGF monoclonal antibodies, such as aflibercept and ranibizumab, represent a line of clinical interventions, approximately 30% of patients show suboptimal therapeutic response [10–12]. Furthermore, the requirements for monthly intravitreal injection of anti-VEGF monoclonal antibodies significantly compromise patient adherence to the treatment [13]. Additionally, long-term use of these drugs may also lead to several complications, including intraocular inflammation and fibrosis [14], necessitating the development of more precise therapeutic approaches.

In recent years, gene silencing technology has provided a promising alternative, with small interfering RNA (siRNA) gaining particular attention due to its advantages of high sequence specificity and precise targeting capabilities [15–17]. siRNA, a type of RNA molecule, plays a crucial role in regulating gene expression. Structurally, siRNA consists of a double-stranded RNA duplex, comprising a guide strand and a passenger strand. The guide strand directs the RNA-induced silencing complex (RISC) to the complementary sequence of the target mRNA molecule, while the passenger strand is generally degraded [18]. Once bound to its target, the guide strand facilitates the formation of an RNA duplex with mRNA, enabling RISC to cleave the target transcript. This cleavage results in mRNA degradation and then silencing of the target gene [19].

Therefore, this study aims to develop a straightforward siRNA formulation suitable for intraocular administration and perform preliminary *in vitro* and *in vivo* experiments to assess its effectiveness and safety.

Materials and Methods

Preparation of siRNA Formulations

Three concentrations of siRNA formulations were prepared. Briefly, 5 mg, 10 mg, and 20 mg siRNA (Sense: GCAGAUUAUGCGGAUCAAACC, Antisense: UUUGAUCCGCAUAAUCUGCAU, Lot. 1162502356, Suzhou Ouli Biomedical Technology Co., Ltd., Suzhou, China) were each dissolved in 1 mL sterile water for injection under continuous stirring. Chitosan (Lot. 21121804, Hunan Xinlvfang Pharmaceutical Co., Ltd., Changsha, China) was dissolved in 0.2 M acetic acid solution (Lot. 20220520, Taicang Hushi Reagent Co., Ltd., Shanghai, China) to prepare a 3 mg/mL solution. One mL of chitosan solution was slowly mixed with each siRNA solution. Appropriate amount of excipients, such as sodium chloride (Lot. 01240404, Tianjin Haiguang Pharmaceutical Co., Ltd., Tianjin, China), were added and dissolved completely. Finally, 1 mL of the high molecular weight hyaluronic acid solution (Kewpie Corporation, Lot. TC22010, Tokyo, Japan) at a concentration of 1 mg/mL was added, and the mixture was stirred for 10 minutes to ensure an entirely homogeneous solution. Employing this protocol, siRNA formulations of low, medium, and high concentrations were prepared for subsequent experiments.

Assessing Rheological Properties of siRNA Formulation

The basic rheological properties of the siRNA formulations were assessed using a rotary rheometer (DHR-1, TA Instruments, USA). An appropriate volume of each siRNA preparation was placed on the Pal plate of the rheometer, and measurements were conducted utilizing a cone-plate rotor in flow shear mode. The measurement temperature was maintained at 25 °C, and the shear rate ranging from 0.1 to 100 s^{-1} was applied to record the flow and viscosity curves for each siRNA preparation.

Cell Culture

Human umbilical vein endothelial cells (HUVECs) (Lot. TCH-C406, Suzhou Haixing Biotechnology Co., Ltd., Suzhou, China) were cultured in DMEM medium (Lot. TCH-GUMD-B318, Suzhou Haixing Biotechnology Co., Ltd., Suzhou, China) containing 10% fetal bovine serum (Lot. TCH-GUMD-R311, Suzhou Haixing Biotechnology Co., Ltd., Suzhou, China) at 37 °C in a humidified incubator with 5% CO_2 (FORMA STERI-CYCLE i160, Thermo Fisher, USA). After achieving approximately 80–90% confluence, cells were washed with phosphate-buffered saline (PBS) (Lot. P1020, Solebo, Beijing, China)

and digested with trypsin (Lot. 25300054, Gibco, New York, USA). After quantification, cells were seeded in culture dishes at a density of 0.75 $\times$ 10^6 cells/mL, with 500 µL per well, and then incubated overnight. Before experiments, HUVEC cells were evaluated for mycoplasma contamination and genetically authenticated using short tandem repeat (STR) profiling by Suzhou Haixing Biotechnology Co., Ltd. Moreover, only mycoplasma-free and genetically authenticated cells were used in subsequent analysis to ensure culture integrity and reproducibility.

Target Dose-Dependent Testing

To assess dose-dependent gene silencing by the corresponding siRNA, different concentrations were tested, and the Half-maximal Inhibitory Concentration (IC_{50}) of the target gene was determined using quantitative reverse transcription polymerase chain reaction (qRT-PCR) (7500, ABI, USA). HUVEC cells were seeded into 96-well plates and transfected with multiple siRNA concentrations (100 nM, 75 nM, 50 nM, 25 nM, 12nM, 6 nM, and 0 nM) prepared by diluting the medium-concentration formulation with PBS, along with transfection reagent (Lot. R19425005, Golden trans technology, Changchun, China). Cells with normal growth were harvested and washed twice with cold PBS, followed by the addition of 1 mL RNA extraction reagent (Lot. R411-01, Vazyme, Nanjing, China). Following RNA extraction, cDNA was prepared, and then the relative expression of the target genes was determined using qRT-PCR Master Mix (Lot. Q312-02, Vazyme, Nanjing, China). Each experiment was performed in triplicate, with *GAPDH* serving as a housekeeping gene. Primers were synthesized by Suzhou Ouli Biomedical Technology Co., Ltd., and their sequences are as follows: vascular endothelial growth factor A-quantitative forward 1 (*VEGFA-Q_F1*): ATCTTCAAGCCATCCTGTG; vascular endothelial growth factor A-quantitative reverse 1 (*VEGFA-Q_R1*): TCATCTCTCCTATGTGCTGG; homo sapiens-glyceraldehyde-3-phosphate dehydrogenase forward 2 (*hs-GAPDH_F2*): CTGGGCTACACTGAGCACC; homo sapiens-glyceraldehyde-3-phosphate dehydrogenase reverse 2 (*hs-GAPDH_R2*): AAGTGGTCGTTGAGGGCAATG. The thermal cycling conditions and melting curve analysis conditions are shown in Table 1. After the reaction, the amplification curve of qRT-PCR was analyzed, and melting curves were simultaneously observed. Relative gene expression was quantified using the $2^{-\Delta\Delta Ct}$ method based on the Ct values, and the data were presented as bar charts.

Table 1. qRT-PCR reaction thermal cycling conditions.

Step	Repeats	Setpoint	Dwell time
Reverse transcription	1	42 °C	30 min
Pre-incubation	1	95 °C	10 min
		95 °C	20 sec
Amplification	45	55 °C	30 sec
		72 °C	30 sec
Melt analysis	Followed the Manufacturer's Manual		

qRT-PCR, quantitative reverse transcription polymerase chain reaction.

CCK-8 Assay

Cell viability was evaluated using the cell counting kit-8 (CCK-8) assay kit (HY-K0301, MCE, USA), following the manufacturer's instructions. HUVEC were seeded into 6-well plates and incubated overnight. The next day, cells were transfected with siRNA at multiple concentrations following an established transfection protocol. Twenty-four hours post-transfection, cells were collected and quantified using a cell counter (Countess3, Invitrogen, USA) and then seeded into 96-well plates at a density of 2 $\times$ 10^3 cells per well. Cell proliferation was assessed at 0, 24, 48, and 72 hours using the CCK-8 reagent, and absorbance was determined at 450 nm (OD value) with a microplate reader (Synergy H1MF, BioTek, USA).

Tube Formation Assay

HUVEC cells were digested and seeded into 6-well plates at a density of 0.75 $\times$ 10^5 cells/mL, with 2000 µL per well, and incubated overnight. The next day, cells were transfected with siRNAs at multiple concentrations. Cells were collected after 24 hours and seeded into 24-well plates precoated with Matrigel (Lot. 356231, Corning, Shanghai, China). After the Matrigel had solidified, 500 µL of the cell suspension was added at a density of 3 $\times$ 10^5 cells per well. Tube formation was observed continuously, and images were captured using an inverted microscope (DMi1, Leica, Germany).

Experimental Animals

Experimental animals, including C57BL/6J mice and rabbits, were purchased from Beijing Weitonglihua Experimental Animal Technology Co., Ltd. (Production License No. SCXK 2021-0006, Beijing, China) and Qingdao Kangdaaibo Experimental Animal Technology Co., Ltd. (Production License No. SCXK (lu) 2021-0023, Qingdao, China), respectively. Animals were housed in individually ventilated cages under a controlled environment of a 12-hour light/dark cycle, with suitable humidity and temperature, and free access to food and water. Efforts were made to minimize animal suffering, including anesthesia by cervical dislocation after anesthesia with injection of Tiletamine Hydrochloride and Zolazepam Hydrochloride for mice and by bloodletting after anesthesia with injection of Tiletamine Hydrochloride and Zolazepam Hydrochloride for rabbits.

Laser-Induced Choroidal Neovascularization Model

C57BL/6J mice (20–24 g, 7–8 weeks old) were anesthetized through intraperitoneal injection of Tiletamine

Hydrochloride and Zolazepam Hydrochloride (Shu Tai™, VIRBAC, Lot. Zoletil 50, French) at a dose of 0.1 mg/kg. The eye designated for injection was disinfected with povidone-iodine solution (H42022671, Hebei Ruikang Pharmaceutical Technology Co., Ltd., Hengshui, China) and topically anesthetized with Obukain hydrochloride eye drops (HJ20215002, Santen, Guangzhou, China), and then the pupils were dilated. The right eye received photocoagulation using a 532 nm argon laser (Vitra, 120 mW power, 0.1 second burst time, spot diameter 100 µm; Ophthalmic Laser Photocoagulation Instrument Quantel Medical, France). The slit lamp light source was adjusted to focus the laser spot on the retina, and four laser burns were applied clockwise around the optic disc. Bubble formation at the burn site indicated Bruch's membrane rupture, confirming successful choroidal neovascularization (CNV) induction [20,21]. On day 0 after laser (D0), a Fundus Fluorescein Angiography (FFA) examination (Heidelberg, Germany) was conducted to evaluate the CNV leakage area. Successful CNV formation was defined as the presence of at least one level-4 fluorescent spot per eye, and mice that met this criterion were grouped according to the size of the CNV area.

Mice were divided into six groups (8 animal per group): a blank group (no injection), a negative control group (normal saline; Lot. 9H85B2, China Otsuka Pharmaceutical Co., Ltd., Tianjin, China), a positive control group (EYLEA, a commercially available anti-VEGF protein drug, 40 mg/mL, S20180010, Germany), and three test groups receiving low, medium, or high concentration of the siRNA preparation. Before treatment, groups were balanced to ensure no significant difference in the size of the CNV leakage area. On day 4 (D4), each mouse in the injection groups, including the negative control, positive control, and test groups, was administered 1 µL of the respective solution using a 31 G microinjection needle (Hamilton, ga33/15mm, Bonaduz, Swiss). The needle was inserted 2–3 mm posterior to the corneal limbus at the temporal 1 o'clock position, with the needle tip oriented towards the optic nerve. Injections were performed gently, and the needle was carefully withdrawn. The injection site was gently pressed with a cotton swab, and ofloxacin eye ointment was applied (H10940177, Xinqi, Shenyang, China) to prevent infection.

FFA was performed on days 7, 21, and 35 (D7, D21, and D35) to evaluate CNV leakage areas. Statistical analysis was conducted to compare treatment efficacy among six groups. After treatment, mice were euthanized after anesthesia with Tiletamine Hydrochloride and Zolazepam Hydrochloride (0.1 mg/kg), through cervical dislocation. Procedures involving animals were approved by the Experimental Animal Ethics Review Committee of Shenyang Xingqi Pharmaceutical Co., Ltd. (IACUC-20240705-0119).

Slit-Lamp and H&E Staining of Retinal Tissue for Drug Safety Evaluation

Drug toxicity and adverse effects were preliminarily evaluated using slit lamp and retinal tissue hematoxylin-eosin (H&E) staining. Twenty-four healthy rabbits (2.0–3.0 kg) were randomly selected and divided into 4 groups (n = 6 per group): a positive control group (PBS, Lot. 2304001, Solarbio, Beijing, China) and three test groups receiving low, medium, and high concentrations of the drugs. Each animal was injected with 0.05 mL of the corresponding formulation via vitreous injection in the right eye.

Slit lamp examination was conducted at 5 and 12 weeks after drug administration. Then, 3 rabbits from each group were euthanized at each time point through bloodletting after anesthesia with Tiletamine Hydrochloride and Zolazepam Hydrochloride (0.1 mg/kg, injected via the ear vein), and retinal tissues were harvested for histopathological examination using H&E staining. All collected eyes were fixed in 10% formalin (Lot. G2160, Solarbio, Beijing, China) for 24 hours. Representative retinal sections were embedded in paraffin, and translucent sections were then stained with H&E (Lot. BL700B, Biosharp, Shanghai, China) for light microscopy assessment.

The animal experiments were approved by the Experimental Animal Ethics Review Committee of Shenyang Xingqi Pharmaceutical Co., Ltd. (IACUC-20230815-78).

Statistical Analysis

Statistical analyses were performed using SPSS 21.0 (IBM Corp., Armonk, NY, USA), with a statistical significance defined at a p-value of <0.05. For normally distributed data, one-way analysis of variance (ANOVA) was applied, whereas nonparametric tests were used for non-normally distributed data. Before statistical analysis, the normality and homogeneity of variance of the datasets were determined using the Shapiro-Wilk test and Levene's test, respectively.

Results

Rheological Analysis of siRNA Formulations

The rheological properties of the formulation can affect drug release, thereby influencing both its effectiveness and safety. Therefore, a basic rheological evaluation was conducted on the siRNA preparations developed in this study. Four siRNA formulations, including low, medium, and high concentrations, along with blank excipient solutions, were assessed for their flow and viscosity features. As shown in Fig. 1, all siRNA formulations demonstrated flow behavior comparable to that of the blank excipient. Furthermore, the viscosity (η) of the siRNA preparations gradually decreased with increasing shear rate, indicating shear-thinning characteristics.

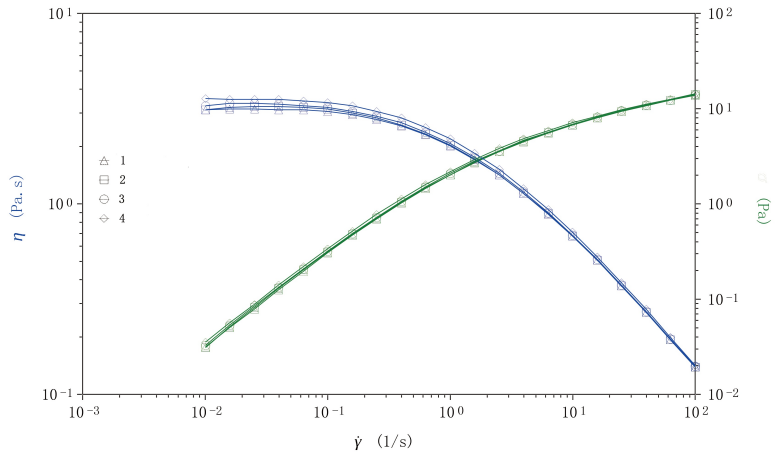

Fig. 1. Rheological characteristic curves of the small interfering RNA (siRNA) formulations (1# blank control group, 2# low test group, 3# medium test group, and 4# high test group).

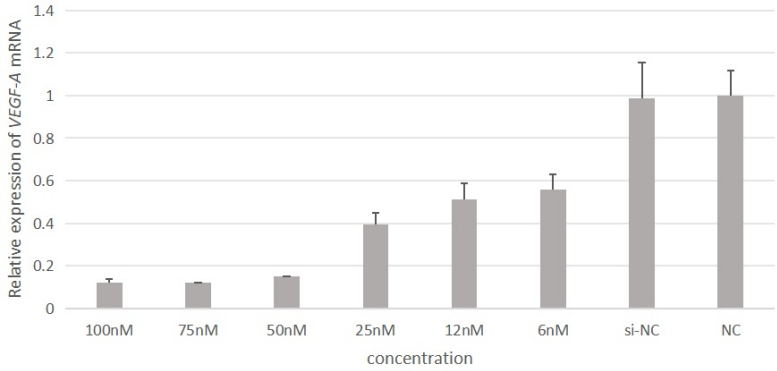

Fig. 2. The knockdown efficiency of siRNA formulations at mRNA levels. *VEGF*, vascular endothelial growth factor; si-NC, negative control siRNA.

Target Dose-Dependent Testing

The effect of VEGF silencing by siRNA formulations was evaluated at the mRNA level using qRT-PCR. HUVEC cells were prepared and seeded into 96-well plates, followed by transfection with siRNA at varying concentrations (100, 75, 50, 25,12, 6, and 0 nM). The finding revealed a dose-dependent silencing of VEGF mRNA, with knockdown efficiency increasing with higher siRNA concentration. The IC_{50} of the siRNA was nearly 12 nM. Furthermore, at 75 nM and 100 nM, VEGF expression was suppressed beyond 85%, confirming the specificity of target silencing. Data are presented as mean ± standard deviation (SD) (n = 3) in Fig. 2.

CCK-8 Assay

Based on qRT-PCR results, siRNA concentrations of 100 nM, 75 nM, and 50 nM were selected for subsequent cellular experiments. Briefly, HUVEC cells underwent overnight incubation in 6-well plates, and were transfected with siRNA at these concentrations, along with a 0 nM control group, following the established procedure. Twenty-four hours post-transfection, cells were collected, counted using a cell counter (Countess3, Invitrogen, USA), and seeded into 96-well plates at a density of 2×10^3 cells per well. After that, cell viability was determined at 0, 24, 48, and 72 hours using the CCK-8 assay with absorbance detected at 450 nm. Relative cell viability was assessed by normalizing the OD value of the treated groups to that of the untreated control group.

The CCK-8 assay results showed that compared to the blank carrier group (BC), cell proliferation was inhibited in all siRNA-treated groups. The siRNA75 nM and 100 nM groups demonstrated similar inhibitory effects. At 24 hours, the siRNA 75 nM and 100 nM groups showed significant inhibition ($p < 0.05$). Similarly, at 48 hours, the siRNA 50 nM group yielded $p < 0.05$, while the siRNA 75 nM and 100 nM groups achieved $p < 0.005$. Furthermore, at 72 hours, the siRNA 50 nM group showed $p < 0.01$, whereas the siRNA 75 nM and 100 nM groups reached $p < 0.005$. The effect of siRNA on cellular viability is shown in Fig. 3.

Tube Formation Assay

The angiogenic capability of HUVEC cells was evaluated using a tube formation assay. During this assay, the ef-

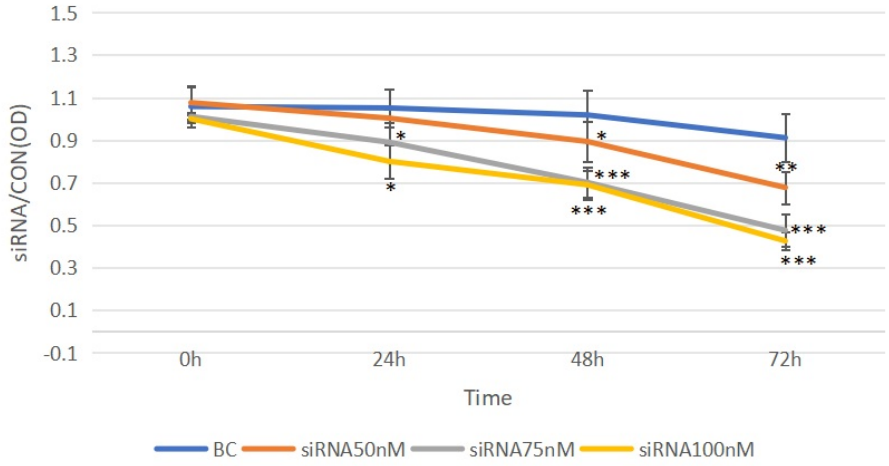

Fig. 3. Impact of vascular endothelial growth factor (VEGF) siRNA on cell viability and proliferation. Test groups value vs. the blank carrier group (BC). Data are presented as mean ± SD of 3 biological replicates. *$p < 0.05$, **$p < 0.01$, ***$p < 0.005$ for each test group vs. the blank carrier group.

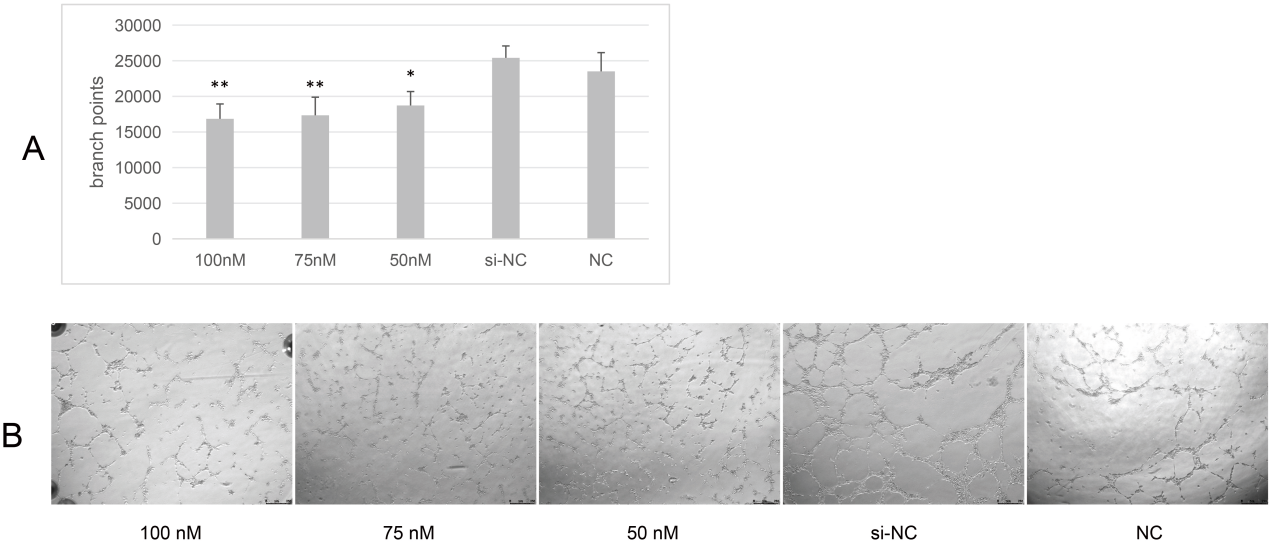

Fig. 4. Impact of VEGF siRNA on the tube formation capability of human umbilical vein endothelial cell (HUVEC). A data bar chart (A) and representative images of the tube formation assay (B). Scale bar: 250 µm. Data are presented as mean ± SD of 3 biological replicates. *$p < 0.05$, **$p < 0.01$ for each test group vs. the NC group.

fects of siRNA at concentrations of 100 nM, 75 nM, and 50 nM were assessed. The blank vector group (si-NC) served as a control, whereas cells without any transfection treatment were used as the negative control (NC).

The findings revealed that the tube-forming capabilities of HUVEC cells were significantly inhibited in all siRNA-treated groups (Fig. 4B), as evidenced by a decrease in total tube length. Furthermore, quantitative analysis confirmed that tube formation was substantially inhibited in all three siRNA-treated groups compared to the NC group (Fig. 4A). In particular, the 50 nM group showed significant inhibition ($p < 0.05$), while the 75 nM and 100 nM groups demonstrated more potent inhibitory effects ($p < 0.01$).

Therapeutic Efficacy of siRNA Formulations on Laser-Induced Choroidal Neovascularization In Vivo

During the experimental period, all mice remained in good general health, showing normal spontaneous activity, clean skin and fur, and no obvious abnormalities in feces or urine. Furthermore, no other toxic reactions related to the test products were observed. Similarly, after administration, no substantial ocular inflammatory responses were observed in the eyes of all mice.

Three days after laser photocoagulation modeling, fluorescence angiography confirmed the successful development of the CNV model in 48 mice across the three experimental groups. At this time point (D3 post-laser), the reti-

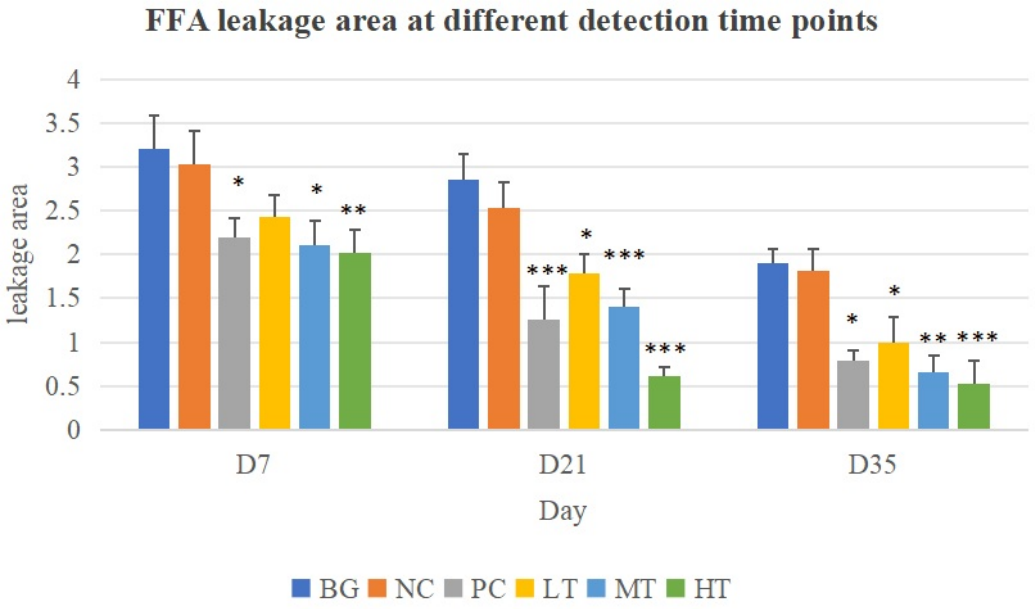

Fig. 5. Assessment of choroidal neovascularization (CNV) leakage area on D7, D21, and D35 post-treatment. Test groups' weekly detection of Fundus Fluorescein Angiography (FFA) leakage area value vs. the NC group FFA leakage area this week. *$p < 0.05$, **$p < 0.01$, ***$p < 0.005$ (n = 8) for each test group vs. the NC group.

nal fundus surrounding the macular region showed a clearly visible laser spot, well-defined fluorescein leakage edges, and leakage at more than one site per eye.

Additionally, FFA was subsequently performed on D7, D21, and D35 to evaluate the CNV leakage area. Therapeutic efficacy was compared across six groups, including a blank group (BG), negative control group (NC), positive control group (PC), low test group (LT), medium test group (MT), and high test group (HT).

We observed that the blank and negative control groups continued to show leakage, whereas the positive control group and all three test groups exhibited a significant reduction in the leakage area. The positive control group and medium test group demonstrated comparable effects, with no statistically significant differences between them. Furthermore, compared to the negative control group, both the positive control group and medium test group yielded $p < 0.05$ on day 7 post-administration, $p < 0.005$ on day 21, and $p < 0.05$ on day 35. However, compared to the negative control group, the high-test group showed $p < 0.01$ on day 7, $p < 0.005$ on day 21, and $p < 0.005$ on day 35. Representative fluorescein angiography findings are shown in Figs. 5,6.

Collectively, these findings indicated that a single intravitreal injection of 1 µL per eye demonstrated significant therapeutic effects in the laser-induced CNV model mice.

Safety Evaluation of siRNA Treatment (Formulations) in Rabbit Retinal Tissue

During these experiments, rabbits were divided into four groups: control group, low-dose group, medium-dose group, and high-dose group. At 5 and 12 weeks after administration, ocular safety was evaluated using slit lamp examination and H&E staining of retinal tissues. As shown in Fig. 7, slit-lamp results revealed no significant inflammation in any group at both time points. Furthermore, H&E staining of retinal tissue (Fig. 8) showed normal morphology across all examined retinal and choroidal layers, no inflammatory structures, pathological abnormalities, or significant intracellular or extracellular edema. These results indicated that the siRNA formulations caused no observable toxicity *in vivo*.

Discussion

In recent years, ocular vascular diseases have remained a significant cause of vision impairment worldwide. Although the emergence of anti-VEGF therapies has provided new hope to patients with ocular angiogenic diseases, the requirement for frequent injections and long-term treatment imposes significant economic and logistical burdens on both patients and the healthcare system. Consequently, there is a growing emphasis on developing novel therapeutics with prolonged efficacy and improved safety profiles.

SiRNA-based therapeutics represent a promising approach due to their high specificity, potent gene-silencing capabilities, and broad target range [22]. However, there are several bottlenecks to realizing the full potential of siRNA-based gene therapy, including chemical instability, non-specific biodistribution, undesirable innate immune responses, and off-target effects [23]. To address these challenges, both viral and non-viral delivery systems have been

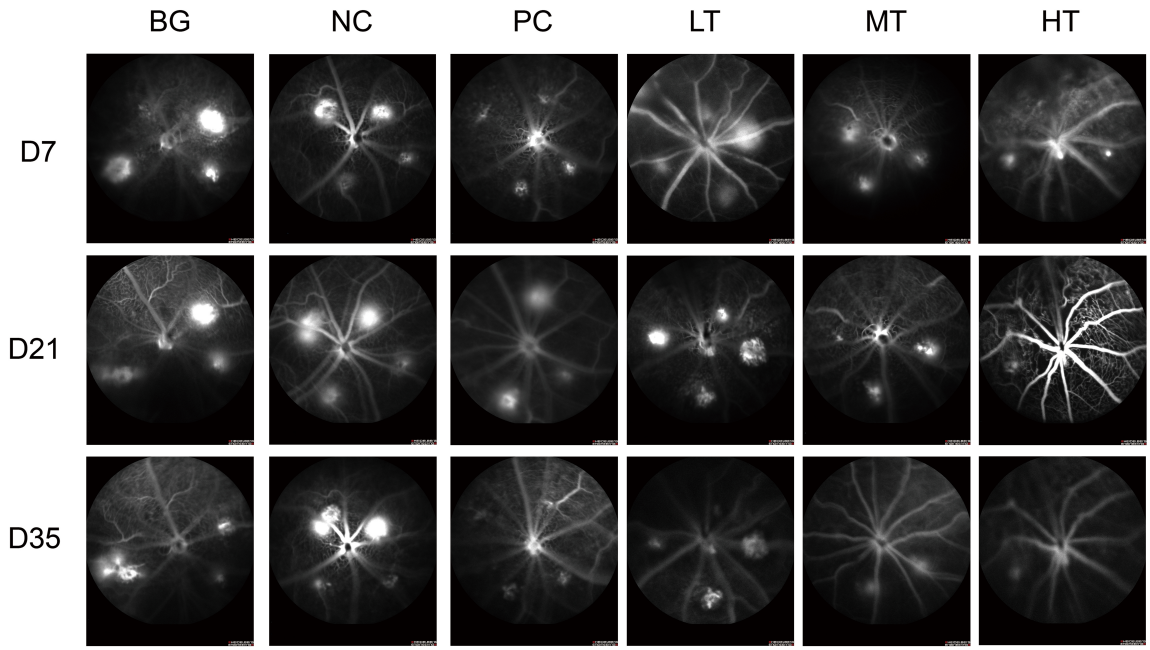

Fig. 6. Representative images after FFA examination on days 7, 21, and 35 (D7, D21, and D35) in each group (n = 8).

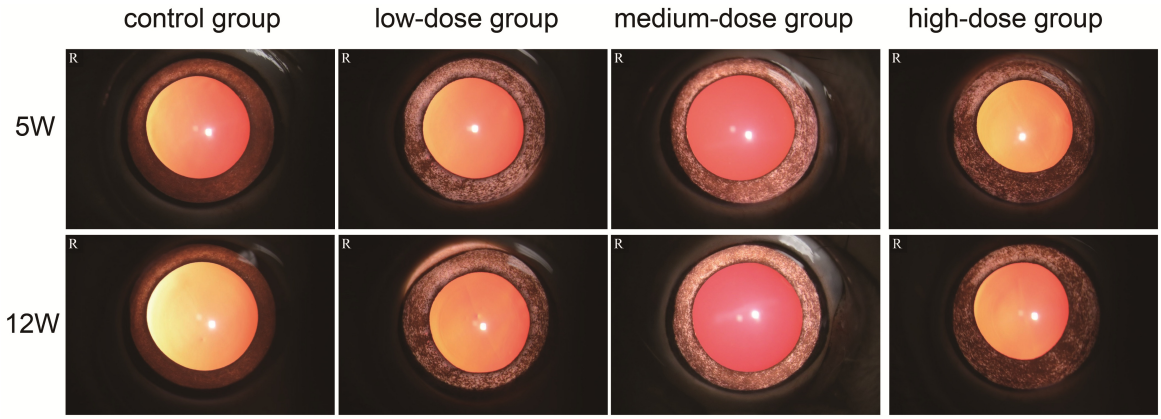

Fig. 7. The results of the slit lamp examination.

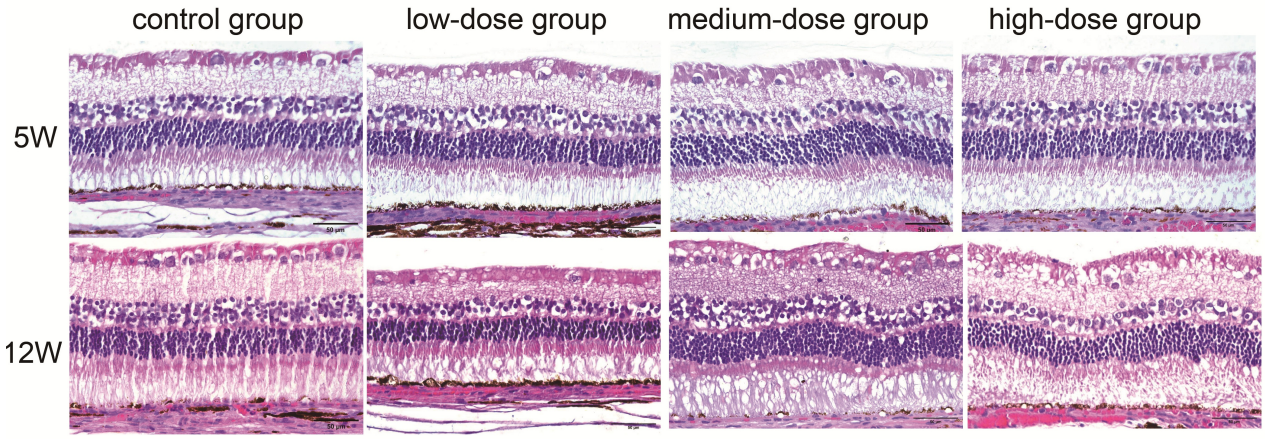

Fig. 8. H&E staining of retinal tissue sections in rabbits at 4 and 12 weeks after intravitreal injection of the siRNA preparations.
Scale bar: 50 μm (n = 3).

explored. Viral vectors, while efficient, pose risks of insertional mutagenesis and activation of oncogene [24,25]. Furthermore, non-viral carriers such as liposomes, polymeric nanoparticles, and inorganic nanomaterials offer advantages, including structural tunability and ease of modification [26]. However, many of these synthetically engineered systems raise concerns regarding biocompatibility, immunogenicity, and long-term toxicity [27,28]. For instance, despite their advantages, liposomes also have some limitations, such as poor stability in biological fluids, opsonization by serum proteins, and potential toxicity associated with certain lipid components [29]. In contrast, the siRNA formulation developed in the current study is composed entirely of pharmacopoeia-approved excipients already employed in marketed intravitreal therapies, thereby minimizing potential toxicity and improving clinical compatibility.

We thoroughly evaluated the efficacy of our novel siRNA formulation through comprehensive *in vitro* and *in vivo* assays, demonstrating several distinct advantages over existing conventional approaches. The VEGFA-targeting siRNA achieved potent and highly specific gene silencing at the mRNA level in HUVECs, as quantified by qRT-PCR. This molecular-level knockdown corresponded to significant functional impairments in angiogenesis-related processes, including alleviated cell proliferation and disrupted tube formation, underscoring the robust anti-angiogenic potential of our formulation.

These findings not only validate but also substantially extend the recent findings reported by Ma *et al*. (2024) [30], who observed comparable VEGF suppression using a polymer-based nanoparticle system. Importantly, our formulation exhibited a significantly improved safety profile, demonstrating no observable cellular toxicity even at higher concentrations—a critical advantage over polymer-based nanoparticles, which showed toxicity at higher doses [30].

Furthermore, in a laser-induced CNV murine model, a single intravitreal injection of our siRNA formulation sustained VEGF suppression for up to five weeks and significantly reduced the CNV area. This durable efficacy represents a major therapeutic improvement over existing anti-VEGF agents, which typically require monthly injections to maintain therapeutic effects. The extended duration of action not only minimizes the treatment burden on patients but also reduces the risk of injection-related complications, positioning our formulation as a highly promising candidate for clinical translation in the treatment of ocular neovascular diseases. Moreover, preliminary safety evaluations conducted via slit-lamp examination and retinal histology revealed no evident toxicities or structural alterations in rabbit eyes over three months.

However, due to limited funding and laboratory conditions, we acknowledge certain limitations in our study. While our preliminary toxicity data demonstrate promising safety profiles, we were unable to assess long-term toxicity effects beyond the 3-month observation period. Particularly, we could not evaluate long-term local effects of siRNA therapy in animals (which would require observing retinal structure and function for over 6 months), conduct functional assessments such as electroretinography (ERG), assess inflammatory markers (e.g., glial fibrillary acidic protein (GFAP) for gliosis), examine carrier-associated toxicity risks, or complete protein-level verification and multi-species validation (including investigations in primates, given the significant anatomical differences between mouse CNV models and human eyes). These challenges will be addressed in future research to support the clinical application of siRNA drugs. Additionally, under prolonged physiological conditions, the *in vivo* stability of siRNA formulations remains poorly elucidated, providing a crucial avenue for future research. While the current formulation demonstrated significant therapeutic effects during the observation period, detailed characterization of siRNA release kinetics will be critical for future formulation optimization and is an ongoing focus of the research group.

In conclusion, our study presents a safe, effective, and clinically viable siRNA formulation utilizing well-established excipients that circumvent many of the toxicity concerns associated with novel synthetic carriers. This approach not only aligns with recent regulatory priorities emphasizing excipient biocompatibility but also offers a promising strategy for enhancing both the safety and efficacy of siRNA delivery platforms. Collectively, these findings offer a meaningful contribution to the field by establishing a new benchmark for non-viral ocular gene therapy formulations.

Conclusion

Overall, our experimental data provide preliminary evidence supporting the therapeutic potential of siRNA formulations targeting VEGF for retinal diseases, underscoring their significance in promoting the clinical translation of siRNA-based therapies in ophthalmology. Hence, future studies should focus on addressing crucial concerns, such as long-term genomic safety, formulation instability, carrier-associated toxicity risks, and other specific limitations.

Availability of Data and Materials

The data that support the findings of this study are available from the corresponding author upon reasonable request.

Author Contributions

LL: Conducting the experiments, collecting and organizing the data, performing statistical analysis, creating the figures and charts, and drafting the initial manuscript. HZX: Formulating the research ideas, designing the experimental methodology, verifying the analytical results,

and overseeing the research progress. Both authors were involved in the drafting and critical revision of the manuscript. Both authors have read and approved the final manuscript. Both authors have participated sufficiently in the work and agreed to be accountable for all aspects of the work.

Ethics Approval and Consent to Participate

All animal experiments were approved by the Institutional Animal Care and Use Committee (IACUC) of Shenyang Xingqi Pharmaceutical Co., Ltd. (CNV: IACUC-20240705-0119; HE: IACUC-20230815-78). All animal experiments were performed following the guidelines of the Experimental Animal Ethics Committee and complied with the Association for Research in Vision and Ophthalmology (ARVO) statement for the Use of Animals in Ophthalmic and Vision Research.

Acknowledgment

Not applicable.

Funding

This research received no external funding.

Conflict of Interest

LL is affiliated with Shenyang Xingqi Pharmaceutical Co., Ltd. The company had no role in the design, execution, or outcomes of this research. The authors declare no other conflicts of interest.

References

[1] Terao R, Kaneko H. Lipid Signaling in Ocular Neovascularization. International Journal of Molecular Sciences. 2020; 21: 4758. https://doi.org/10.3390/ijms21134758.

[2] Fleckenstein M, Schmitz-Valckenberg S, Chakravarthy U. Age-Related Macular Degeneration: A Review. JAMA. 2024; 331: 147–157. https://doi.org/10.1001/jama.2023.26074.

[3] Pieńczykowska K, Bryl A, Mrugacz M. Link Between Metabolic Syndrome, Inflammation, and Eye Diseases. International Journal of Molecular Sciences. 2025; 26: 2174. https://doi.org/10.3390/ijms26052174.

[4] Teo ZL, Tham YC, Yu M, Chee ML, Rim TH, Cheung N, *et al*. Global Prevalence of Diabetic Retinopathy and Projection of Burden through 2045: Systematic Review and Meta-analysis. Ophthalmology. 2021; 128: 1580–1591. https://doi.org/10.1016/j.ophtha.2021.04.027.

[5] James LM. Age-related macular degeneration. Nursing. 2024; 54: 50–53. https://doi.org/10.1097/NSG.0000000000000079.

[6] Song M, Yang H, Yao S, Ma F, Li Z, Deng Y, *et al*. A critical role of vascular endothelial growth factor D in zebrafish embryonic vasculogenesis and angiogenesis. Biochemical and Biophysical Research Communications. 2007; 357: 924–930. https://doi.org/10.1016/j.bbrc.2007.04.033.

[7] Sheth JU, Stewart MW, Narayanan R, Anantharaman G, Chandran K, Lai TYY, *et al*. Macular neovascularization. Survey of Ophthalmology. 2025; 70: 653–675. https://doi.org/10.1016/j.survophthal.2024.08.003.

[8] Guo Z, Jing X, Sun X, Sun S, Yang Y, Cao Y. Tumor angiogenesis and anti-angiogenic therapy. Chinese Medical Journal. 2024; 137: 2043–2051. https://doi.org/10.1097/CM9.0000000000003231.

[9] Shellvarajah M, Nguyen V, Steinmann S, Gillies MC, Sagkriotis A, Barthelmes D. Adherence to Anti-VEGF Treatment in Patients with Neovascular Age-Related Macular Degeneration: A Real-World Study. Ophthalmology and Therapy. 2025; 14: 1261–1269. https://doi.org/10.1007/s40123-025-01140-z.

[10] Shirian JD, Shukla P, Singh RP. Exploring new horizons in neovascular age-related macular degeneration: novel mechanisms of action and future therapeutic avenues. Eye. 2025; 39: 40–44. https://doi.org/10.1038/s41433-024-03373-x.

[11] Borrelli E, Foti C, Ulla L, Porreca A, Introini U, Grassi MO, *et al*. Incidence and reasons for discontinuation of anti-VEGF treatment in neovascular age-related macular degeneration. The British Journal of Ophthalmology. 2025; 109: 875–881. https://doi.org/10.1136/bjo-2024-326152.

[12] Yan A, Jones C, Demirel S, Chhablani J. Diabetic macular edema: Upcoming therapies. Graefe's Archive for Clinical and Experimental Ophthalmology. 2025; 263: 249–258. https://doi.org/10.1007/s00417-024-06595-7.

[13] Kuo BL, Singh RP. Brolucizumab for the treatment of diabetic macular edema. Current Opinion in Ophthalmology. 2022; 33: 167–173. https://doi.org/10.1097/ICU.0000000000000849.

[14] Cox JT, Eliott D, Sobrin L. Inflammatory Complications of Intravitreal Anti-VEGF Injections. Journal of Clinical Medicine. 2021; 10: 981. https://doi.org/10.3390/jcm10050981.

[15] Guimaraes TACD, Georgiou M, Bainbridge JWB, Michaelides M. Gene therapy for neovascular age-related macular degeneration: rationale, clinical trials and future directions. The British Journal of Ophthalmology. 2021; 105: 151–157. https://doi.org/10.1136/bjophthalmol-2020-316195.

[16] Supe S, Upadhya A, Singh K. Role of small interfering RNA (siRNA) in targeting ocular neovascularization: A review. Experimental Eye Research. 2021; 202: 108329. https://doi.org/10.1016/j.exer.2020.108329.

[17] Li T, Wang Y, Chen X, Cui H, Zhang L, Liu J, *et al*. Direct Cytosolic Delivery of siRNA Conjugates: A Paradigm in Antiangiogenic Therapy for Choroidal Neovascularization. ACS Nano. 2025; 19: 11249–11262. https://doi.org/10.1021/acsnano.4c18924.

[18] López-Fraga M, Martínez T, Jiménez A. RNA interference technologies and therapeutics: from basic research to products. BioDrugs: Clinical Immunotherapeutics, Biopharmaceuticals and Gene Therapy. 2009; 23: 305–332. https://doi.org/10.2165/11318190-000000000-00000.

[19] Medley JC, Panzade G, Zinovyeva AY. microRNA strand selection: Unwinding the rules. Wiley Interdisciplinary Reviews. RNA. 2021; 12: e1627. https://doi.org/10.1002/wrna.1627.

[20] Park JR, Choi W, Hong HK, Kim Y, Jun Park S, Hwang Y, *et al*. Imaging Laser-Induced Choroidal Neovascularization in the Rodent Retina Using Optical Coherence Tomography Angiography. Investigative Ophthalmology & Visual Science. 2016; 57: OCT331-40. https://doi.org/10.1167/iovs.15-18946.

[21] Lin JB, Apte RS. The Landscape of Vascular Endothelial Growth Factor Inhibition in Retinal Diseases. Investigative Ophthalmology & Visual Science. 2025; 66: 47. https://doi.org/10.1167/iovs.66.1.47.

[22] Setten RL, Rossi JJ, Han SP. The current state and future directions of RNAi-based therapeutics. Nature Reviews. Drug Discovery. 2019; 18: 421–446. https://doi.org/10.1038/s41573-019-0017-4.

[23] Kurakula H, Vaishnavi S, Sharif MY, Ellipilli S. Emergence of Small Interfering RNA-Based Gene Drugs for Various Diseases.

ACS Omega. 2023; 8: 20234–20250. https://doi.org/10.1021/acsomega.3c01703.

[24] Li X, Le Y, Zhang Z, Nian X, Liu B, Yang X. Viral Vector-Based Gene Therapy. International Journal of Molecular Sciences. 2023; 24: 7736. https://doi.org/10.3390/ijms24097736.

[25] Zu H, Gao D. Non-viral Vectors in Gene Therapy: Recent Development, Challenges, and Prospects. The AAPS Journal. 2021; 23: 78. https://doi.org/10.1208/s12248-021-00608-7.

[26] Picanço-Castro V, Pereira CG, Covas DT, Porto GS, Athanassiadou A, Figueiredo ML. Emerging patent landscape for non-viral vectors used for gene therapy. Nature Biotechnology. 2020; 38: 151–157. https://doi.org/10.1038/s41587-019-0402-x.

[27] Witwer KW, Wolfram J. Extracellular vesicles versus synthetic nanoparticles for drug delivery. Nature Reviews. Materials. 2021; 6: 103–106. https://doi.org/10.1038/s41578-020-00277-6.

[28] Mitchell MJ, Billingsley MM, Haley RM, Wechsler ME, Peppas NA, Langer R. Engineering precision nanoparticles for drug delivery. Nature Reviews. Drug Discovery. 2021; 20: 101–124. https://doi.org/10.1038/s41573-020-0090-8.

[29] Subhan MA, Filipczak N, Torchilin VP. Advances with Lipid-Based Nanosystems for siRNA Delivery to Breast Cancers. Pharmaceuticals. 2023; 16: 970. https://doi.org/10.3390/ph16070970.

[30] Ma X, Cui Y, Zhang M, Lyu Q, Zhao J. A Multifunctional Nanodrug Co-Delivering VEGF-siRNA and Dexamethasone for Synergistic Therapy in Ocular Neovascular Diseases. International Journal of Nanomedicine. 2024; 19: 12369–12387. https://doi.org/10.2147/IJN.S492363.